

## THE ORIGIN AND EVOLUTION OF THE MASS-METALLICITY RELATIONSHIP FOR GALAXIES: RESULTS FROM COSMOLOGICAL N-BODY SIMULATIONS

A. M. BROOKS<sup>1,2</sup>, F. GOVERNATO<sup>1</sup>, C. M. BOOTH<sup>3</sup>, B. WILLMAN<sup>4,5</sup>, J. P. GARDNER<sup>6</sup>, J. WADSLEY<sup>7</sup>, G. STINSON<sup>1</sup>, T. QUINN<sup>1</sup>

*Draft version October 16, 2019*

### ABSTRACT

We examine the origin and evolution of the mass-metallicity relationship ( $M_*$ - $Z$ ) for galaxies using high resolution cosmological SPH + N-Body simulations that include a physically motivated description of the effects of supernovae feedback and subsequent metal enrichment. Our simulations allow us to distinguish between two possible sources that contribute to both the origin of the mass-metallicity relationship and to the low chemical yield observed at low galaxy masses: 1) metal and baryon loss due to gas outflow, or 2) inefficient star formation at the lowest galaxy masses. Our simulated galaxies reproduce the observed  $M_*$ - $Z$  relationship in shape and normalization both at  $z=0$  and  $z=2$ . We show that low star formation efficiencies, regulated by supernovae feedback, are primarily responsible for the lower metallicities of low mass galaxies and the overall  $M_*$ - $Z$  trend. We find that the shape of the  $M_*$ - $Z$  relation is relatively constant with redshift, but that its normalization increases with time. Simulations with no energy feedback from supernovae overproduce metals at low galaxy masses by rapidly transforming a large fraction of their gas into stars. We find that gas mass loss due to supernovae induced winds and the cosmic UV field becomes significant in our galaxies with  $M_{bar} < 10^8 M_\odot$ . Some gas loss due to supernovae feedback is necessary to reproduce the observed low effective yield observed in low mass galaxies. Despite the fact that our low mass galaxies have lost a majority of their baryons, they are still the most gas rich objects in our simulations due to their low star formation efficiencies.

*Subject headings:* galaxies: evolution — galaxies: formation — methods: N-Body simulations

### 1. INTRODUCTION

The observed trend that the metallicity of nearby galaxies decreases with galaxy mass has been well established in the literature (e.g., Tremonti et al. 2004; Lee et al. 2006). This trend has also recently been observed at high redshifts (Savaglio et al. 2005; Erb et al. 2006). The gas metallicity of a galaxy depends on reprocessed material from its stars and subsequent inflow and outflow of gas. The mass-metallicity relationship thus provides insight into two physical mechanisms important to the evolution of galaxies: star formation efficiency and gas inflow/outflow.

In a “closed box” system (no inflow or outflow of material), metallicity  $Z$  is given by

$$Z = y \ln f_{gas}^{-1}, \quad (1)$$

where  $y$  is the nucleosynthetic metal yield produced by stars and  $f_{gas}$  is the gas mass fraction ( $M_{gas}/[M_{gas} + M_{stars}]$ ) (e.g., Tinsley 1980). In general, low mass galaxies are observed to have higher gas fractions than high mass galaxies (e.g., Geha et al. 2006; West 2005). This observation can easily explain the origin of the  $M_*$ - $Z$  relation in the context of the closed

box model. In this scenario, low mass galaxies are gas rich because they are inefficient at turning gas into stars, likely due to their low surface densities (Kennicutt 1998; Martin & Kennicutt 2001; Verde et al. 2002; Dalcanton et al. 2004). Governato et al. (2006) and Stinson et al. (2006) showed that energy injection from supernovae (SNe) feedback can act to lower the star formation (SF) efficiency.

The second effect of SNe feedback might be to expel gas in galactic winds. In this scenario the loss of metals becomes progressively more important at lower masses due to shallower halo potential wells and leads to the observed  $M_*$ - $Z$  trend. SNe feedback has been the favored explanation for enriched intergalactic and intracluster gas (for a review see Veilleux et al. 2005). Additionally, feedback has been invoked to explain the lack of visible low mass satellite halos in the local neighborhood (e.g., White & Frenk 1991; Kauffmann et al. 1993; Moore et al. 1999). However, the importance of supernova feedback as a function of galaxy mass has been investigated by various groups, with results that are still debated (Veilleux et al. 2005; Geha et al. 2006; Erb et al. 2006; Dalcanton 2006).

Recently, studies have investigated how the  $M_*$ - $Z$  relation evolves with cosmic time (Savaglio et al. 2005; Erb et al. 2006; Davé et al. 2006; De Rossi et al. 2006; Kobayashi et al. 2006; Tassis et al. 2006). Fully cosmological numerical experiments are one of the best tools to infer the relative importance of star formation (SF) and feedback processes in a realistic setting (e.g., Okamoto et al. 2005; Robertson et al. 2006; Governato et al. 2006, hereafter G06) where the complexity of dark matter and gas interaction and accretion are followed in full detail. In this Letter, we investigate

<sup>1</sup> Astronomy Department, University of Washington, Box 351580, Seattle, WA, 98195-1580

<sup>2</sup> e-mail address: abrooks@astro.washington.edu

<sup>3</sup> Department of Physics, Institute for Computational Cosmology, University of Durham, South Road, Durham, DH1 3LE, UK

<sup>4</sup> Harvard-Smithsonian Center for Astrophysics, 60 Garden Street, Cambridge, MA, 02138

<sup>5</sup> Clay Fellow

<sup>6</sup> Department of Physics & Astronomy, University of Pittsburgh, 100 Allen Hall, 3941 O’Hara Street, Pittsburgh, PA, 15260

<sup>7</sup> Department of Physics and Astronomy, McMaster University, Hamilton, Ontario, L8S 4M1, Canada

the origin and evolution of the mass-metallicity relation in a concordance  $\Lambda$ CDM cosmological setting with N-body + SPH simulations where a physically motivated treatment of the effects SF and SN feedback are included. The simulations in this paper have some of the highest mass and force resolution run to date, and allow us to study the formation history of galaxies over an extended range of masses, and thus quantify the importance of feedback and blowout versus low SF efficiencies over their lifetimes.

## 2. THE SIMULATIONS

We selected four “field” regions ( $d\rho/\rho \sim 0.1$ ) from a low resolution, dark matter simulation run in GASOLINE (Wadsley et al. 2004) using a concordance, flat,  $\Lambda$ -dominated cosmology:  $\Omega_0 = 0.3$ ,  $\Lambda=0.7$ ,  $h = 0.7$ ,  $\sigma_8 = 0.9$ , shape parameter  $\Gamma = 0.21$ , and  $\Omega_b = 0.039$  (Perlmutter et al. 1997; Efstathiou et al. 2002). These “field” regions were resimulated at higher resolution using the volume renormalization technique (Katz & White 1993), which allows us to resolve fine structure while capturing the effect of large scale torques. The “field” regions are centered around galaxies with peak rotation velocity  $V_{rot} \sim 150$  and  $275$  km/s, with each high resolution region having a comoving volume of  $\sim 100$ – $1000$  Mpc<sup>3</sup>. Two of the main galaxies are described in detail in G06, although for this study they have been rerun at higher resolution. At  $z=0$ , these three runs yield a sample of 32 high resolution disk and dwarf galaxies over a range of peak velocities  $30$  km/s  $< V_{rot} < 275$  km/s, or total halo masses from  $3.4 \times 10^9 M_\odot$  to  $1.1 \times 10^{12} M_\odot$ . Seven of these 32 galaxies are satellites of the primaries.

Our best runs have particle masses of  $7.6 \times 10^5 M_\odot$ ,  $1.3 \times 10^5 M_\odot$ , and  $3.8 \times 10^4 M_\odot$  for DM, gas, and stars, respectively, and a force resolution (spline softening) of  $0.3$  kpc. These simulations include a simple but physically motivated recipe (full details in Stinson et al. 2006) to describe SF and the effects of subsequent SNe feedback. The supernova efficiency parameter  $\epsilon_{SN}$  was set to  $0.4$  and SF efficiency  $c_* = 0.05$ , as in G06, with an IMF from Kroupa et al. (1993). Metal enrichment from both SN Ia&II is followed based on the prescription of Raiteri et al. (1996), who adopt yields from Thielemann et al. (1986) for SN Ia, and Weaver & Woosley (1993) and Woosley & Weaver (1995) for SN II.

As discussed in G06, at  $z=0$  disk galaxies in our simulations fall on the Tully-Fisher (TF) and baryonic TF relations (Giovanelli et al. 1997; McGaugh 2005) and the age-mass relation (MacArthur et al. 2004). Our adopted SN feedback and cosmic UV background (Haardt & Madau 1996) also drastically reduce the number of galaxy satellites containing a significant stellar population, making many of them “dark” (Moore et al. 1999). Galaxies and their parent halos were identified using AHF<sup>8</sup> (Knebe et al. 2001; Gill et al. 2004).

## 3. THE ORIGIN OF THE MASS-METALLICITY RELATION

The mass-metallicity relationship for 32 high resolution galaxies in our simulations is shown in Fig. 1, at

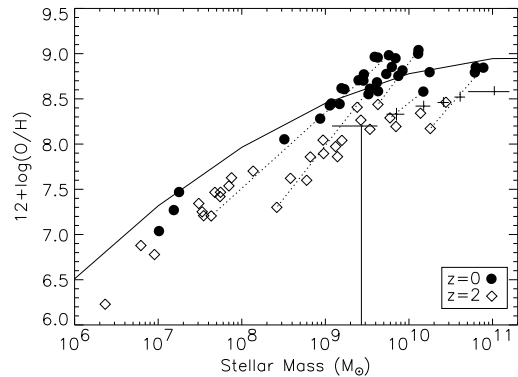


FIG. 1.— The mass-metallicity relation of our simulated galaxies at  $z=0$  (solid points) and  $z=2$  (open diamonds). The solid curved line is the observational fit to  $>53,000$  galaxies in SDSS from T04. Error bars show the observational mass-metallicity relation at  $z=2$  from E06. Dotted lines connect some of the  $z=0$  galaxies to their progenitors at  $z=2$ , showing how galaxies evolve in the  $M_*$ - $Z$  plane with time.

both  $z=0$  and  $z=2$ . The solid curved line is the empirical fit for  $> 53,000$  galaxies in SDSS from Tremonti et al. (2004, hereafter T04). It has been shifted down by  $0.2$  dex to account for the fact that the method used by T04 is known to systematically find O abundances up to  $0.3$  dex larger than other methods (T04, Savaglio et al. 2005; Erb et al. 2006; Lee et al. 2006). The galaxies in our sample at  $z=0$  match the empirical fit of T04 extremely well, reproducing the observed trend over almost 4 orders of magnitude in stellar mass. We note that our lowest mass galaxies, however, have a lower O abundance than that found for dwarf irregular galaxies by Lee et al. (2006).

Fig. 1 also shows that the mass-metallicity relation for our simulated galaxies at  $z=2$  (open diamonds) is in excellent agreement with high redshift data. The error bars overplotted on Fig. 1 display the observational results from Erb et al. (2006, hereafter E06) and occupy the same region of the  $M_*$ - $Z$  plane as our simulated galaxies at  $z=2$ . We have identified in the simulations the  $z=0$  galaxies corresponding to those plotted at  $z=2$ . The dotted lines in Fig. 1 connect a few of these galaxies, which are representative of how all the galaxies have evolved in the  $M_*$ - $Z$  plane with time.

The O abundances for our data points shown in Fig. 1 are derived from cool gas particles (with temperature  $< 40,000$  K) in our simulations. The SDSS fibers lead to a sampling of only the inner portions of large, nearby galaxies in the T04 sample. To make a meaningful comparison with our  $z=0$  sample, we only included cool gas within  $2.5$  kpc of each simulated galaxy center. At  $z=2$  we included all cold gas in each galaxy. For the few highest mass galaxies at  $z=0$ , using all of the cool gas generally lowers the derived O abundance by  $0.2$ – $0.5$  dex because of radial metallicity gradients in galaxy disks. Even including all cool gas, the  $M_*$ - $Z$  trend is unchanged up to  $10^{10} M_\odot$ , showing that the evolution seen in Fig. 1 is not an effect of our measurements.

A few runs were repeated at lower resolutions ( $1/2$  and  $1/20$  of the mass resolution). Low resolution runs undergo less SF (likely as the dynamic range of the gas component is reduced as its particle mass increases) thus

<sup>8</sup> AMIGA’s Halo Finder, available for download at <http://www.aip.de/People/aknebe/AMIGA>

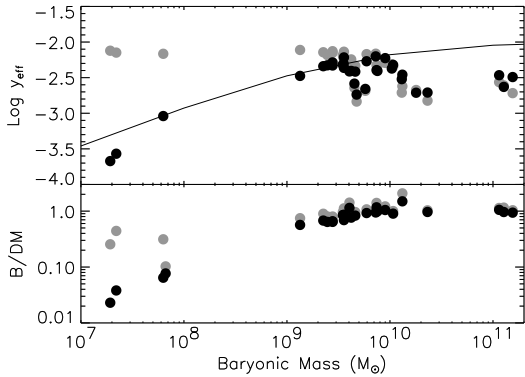


FIG. 2.— *Top Panel:* Effective yield vs total baryonic mass for our galaxies based on the inner cold gas phase O abundance at  $z=0$  (black circles). The solid curved line is the observational fit to  $>53,000$  galaxies from T04. *Bottom Panel:* Baryonic to dark matter mass ratio (relative to the cosmic abundance) vs total baryonic mass. Satellite galaxies excluded. In both panels, grey circles show what the value would be if no gas loss from the galaxies had occurred.

decreasing both  $M_*$  and the total amount of O produced. Our results from each run begin to significantly diverge from each other ( $\Delta M_* > 20\%$ ,  $\Delta 12+\log(\text{O}/\text{H}) > 0.2$  dex) if the number of DM particles in a halo drops below a few thousand and/or mass and force resolution degrade too much. Note that this low resolution effect can lead to an artificial  $M_*$ - $Z$  trend, making it essential that results converge. Informed by these resolution tests, we have only included galaxies with more than 3500 DM particles in our sample (at high and low redshift), ensuring that their stellar and metal content have converged.

Having shown that our simulations reproduce the observed  $M_*$ - $Z$  relation at both  $z=0$  and  $z=2$ , we will next examine the origin of this relation. The resolution of our simulations allows us to trace gas in our galaxies as it enters and leaves a system, and thus quantify the importance of preferential metal loss at low masses versus low SF efficiency in producing the mass-metallicity relationship.

### 3.1. The Role of Mass Loss

To determine if gas mass loss plays a role in the shape of the  $M_*$ - $Z$  relation, we have traced all the gas particles that ever belonged to our galaxies back to  $z=3$ . We define lost gas as gas outside of the  $z=0$  virial radius of its former parent galaxy. When all gas (remaining + lost) is considered, we find that only the three lowest mass galaxies have a higher O abundance than compared to the remaining cold gas at  $z=0$ . However, the increase in O is less than 0.3 dex in all cases because the lost gas has roughly the same O abundance as the remaining cool gas. The overall trend that lower mass galaxies have lower metallicities still exists, and it cannot be mass loss alone that causes the  $M_*$ - $Z$  relation.

Another observable quantity commonly used to investigate mass loss from galaxies is the effective yield,  $y_{eff}$ . From Eq. 1, we can define the effective yield,

$$y_{eff} = Z/(\ln f_{gas}^{-1}). \quad (2)$$

In a closed box system,  $y_{eff}$  is equal to the true stellar nucleosynthetic yield, but it can be inferred from Eq. 2

that  $y_{eff}$  may deviate from the true yield due to inflow or outflow of gas. The top panel of Fig. 2 shows  $y_{eff}$  for our galaxies, derived again using inner cold gas abundances, versus the total baryonic mass of our galaxies at  $z=0$  (black circles). The effective yields reproduce the observed trend from T04 over most of our mass range (solid line). Our two lowest mass galaxies have  $y_{eff}$  below that found by Lee et al. (2006), likely because these two have undergone additional tidal stripping of gas.

The bottom panel of Fig. 2 shows the baryonic to dark mass ratio (B/DM) of our galaxies (the seven satellite galaxies have been excluded from this panel), with respect to the cosmic abundance. In our simulations, large deviations below  $B/DM = 1$  can only be produced by gas loss. Our lowest mass galaxies have lost up to 98% of their baryonic mass (black circles).

When we include all of the gas lost more recently than  $z = 3$ , we find that our low mass galaxies still have B/DM that fall significantly below the cosmic abundance. The grey points in the bottom panel of Figure 2 show that our lowest mass galaxies have lost 50 - 90% of their baryons prior to  $z = 3$ . To achieve the flat  $y_{eff}$  trend seen in the top panel of Fig. 2 in the event of such significant mass loss requires that this mass was lost prior to the advent of SF in these galaxies, for example by heating from the UV background. We verify that a UV only simulation (SNe feedback turned off) removes up to 80% of baryons from our lowest mass galaxies, but that these galaxies evolve as closed boxes once SF commences. Using simulated low mass galaxies that have evolved in isolation and comparing runs with and without SN feedback, we thus find that SNe induced mass loss can account for up to 20% of baryon loss from galaxies with  $M_{bar} < 1 \times 10^8 M_\odot$ . Additional gas loss can occur via tidal stripping.

### 3.2. Star Formation Efficiencies

As explained above, the mass loss experienced by our lowest mass galaxies cannot account for the shape of the  $M_*$ - $Z$  relation. We now investigate whether SF efficiencies can explain the origin of this trend. If lower mass galaxies convert gas into stars less efficiently than higher mass galaxies, then they will require a much longer period of time to enrich the remaining gas to the same metallicity as higher mass galaxies. This effect can lead to the observed  $M_*$ - $Z$  relationship, with or without mass loss as an additional contributor.

All of our galaxies follow the Schmidt-Kennicutt law for SF (Kennicutt 1998; Martin & Kennicutt 2001). Our galaxies span a factor of 250 in gas surface densities, yielding a SFR that varies by over three orders of magnitude from our lowest to highest mass galaxies. Our lowest mass galaxies are thus incredibly inefficient at SF when compared to our high mass galaxies. The consumption rate ( $\text{SFR}/M_{coldgas}$ ) of our lowest mass galaxies is about two orders of magnitude lower than our highest mass galaxies. That is, while our highest mass galaxies will use up all their gas in 1 Gyr or less, our lowest mass galaxies will take up to 60 Gyr if they continue SF at their current rate.

Fig. 3 shows the gas mass fraction,  $f_{gas}$ , versus rotational velocity for our galaxies (satellite galaxies excluded). As found by recent observations of isolated galaxies (e.g, West 2005; Geha et al. 2006), lower mass galaxies have increasing gas fractions, implying that

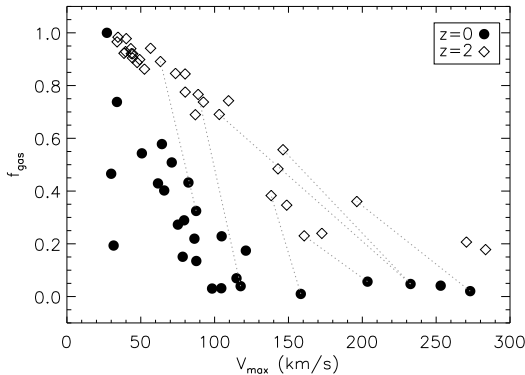


FIG. 3.— The gas mass fraction vs  $V_{rot}$  for our galaxies at  $z=0$  and  $z=2$  (satellite galaxies excluded). Faint dotted lines connect a few of the galaxies at  $z=2$  to their evolved counterpart at  $z=0$ .

lower mass galaxies have been less efficient at making stars. Note that while the lowest mass galaxies in our sample have lost more than 90% of their baryons (Fig. 2), they remain gas rich due to their low SF efficiencies (with the exception of two that have been tidally stripped of much of their gas).

We reran our simulations without SNe feedback. In the absence of such feedback, the  $M_*$ - $Z$  relation is flat because low mass galaxies experience unrealistically high star formation rates, resulting in an overproduction of metals. This difference with the runs that do include SNe demonstrates that energy injection by SNe into the ISM regulates star formation efficiency, independent of whether SNe also lead to mass loss. SNe feedback thus indirectly affects the shape of the  $M$ - $Z$  relation by modulating the gas surface densities, and hence the SFR, with galaxy mass.

#### 4. THE EVOLUTION OF THE MASS-METALLICITY RELATION

Fig. 3 shows that our simulated galaxies at  $z=2$  are less evolved than their  $z=0$  counterparts, with  $z=2$  galaxies being much more gas rich at a given rotational velocity than at  $z=0$ . By  $z=0$ , they have consumed more of their gas, increasing both their stellar mass and O abundance; hence the evolution of the  $M_*$ - $Z$  relation as shown in Fig. 1. Both Savaglio et al. (2005, hereafter S05) and E06 examined the  $M_*$ - $Z$  relation at  $z\sim 0.7$  and  $z\sim 2$ , respectively, and drew similar conclusions. As pointed out by S05 and Pettini (2006), at a given metallicity the high  $z$  data are about an order of magnitude more massive than the  $z=0$  trend (Fig. 1). This suggests that more massive galaxies enrich at a faster rate than lower mass galaxies. This is supported by our results in section 3.2.

Both S05 and E06 conclude that the evolution of the  $M_*$ - $Z$  relation is best described by a model in which low mass galaxies are inefficient at SF relative to high mass galaxies for a similar formation epoch. Thus the period of SF is lengthened in lower mass galaxies and they remain more gas rich at a given redshift. However, E06 find that their data are best fit by a model with strong mass outflow, while S05 find that a closed box model can evolve their galaxies onto the  $z\sim 0$  relation of T04. As discussed in 3.1, a small amount of baryons (up to 20%) have been lost due to SNe winds in our lowest mass galaxies.

We find that a shift downward by 0.6 dex in  $\Delta\log(\text{O}/\text{H})$  from the best fit  $M_*$ - $Z$  relation found by T04 is an excellent fit to our  $z=2$  data. A shift in  $\Delta\log(M_*)$  is much too steep to match our simulations. Thus, we find that the slope of the  $M_*$ - $Z$  relation remains relatively constant with redshift, but the normalization increases with time.

#### 5. CONCLUSIONS

We have presented results from high resolution simulations of field galaxies in a  $\Lambda$ CDM context. The simulations are carried to  $z=0$  and include SF and a physically motivated description of the effects of SNe feedback and metal enrichment. We have shown in previous work (G06) that this approach leads to disk galaxies that fall on the TF and baryonic TF relations and reproduce the age-mass relation and abundance of galaxy satellites. Here we present a natural extension of this analysis, showing that the simulated galaxies are also in excellent agreement with the observed  $M_*$ - $Z$  relation both at  $z=0$  and  $z=2$ .

Simulated galaxies match both the slope and normalization of the  $M_*$ - $Z$  relation over a range of four orders of magnitude in stellar mass. We find that the slope of the  $M_*$ - $Z$  relation is roughly constant with redshift, but that its normalization increases with time. Such evolution agrees with the high- $z$  observations of Erb et al. (2006), and with early theoretical predictions (Davé et al. 2006; De Rossi et al. 2006). Furthermore, the mass scales of the turnovers in our simulated  $Z$ ,  $y_{eff}$ , B/DM, and  $f_{gas}$  versus mass relations are in good agreement with a range of previous observational and theoretical studies that find critical transitions at  $\sim 120$  km/s (e.g., Dalcanton et al. 2004; Kereš et al. 2005; Dekel & Birnboim 2006).

Galaxies with  $M_{bar} < 10^8 M_\odot$  ( $V_{rot}\sim 50$  km/s), lose a significant amount of their baryons due to combined heating from the cosmic UV field and SN feedback. Baryon loss due to SN feedback results in a  $y_{eff}$ - $M_{bar}$  trend in agreement with the results from the SDSS (T04). However, including gas that has been lost from galaxies does not alter the O abundances significantly, and does not change the overall shape of the  $M_*$ - $Z$  relation, confirming that the lower O abundances in our low mass galaxies are primarily due to their low SF efficiencies rather than directly to blowouts. Despite strong baryon loss from their halos, we find that our cold gas fractions at low galaxy masses are in qualitative agreement with recent observational samples (Geha et al. 2006).

SN feedback plays a crucial role in lowering the SF efficiency in low mass galaxies and originating the turnover in the  $M_*$ - $Z$  relation at the observed scales. Without energy injection from SNe to regulate SF, gas that remains in galaxies rapidly cools, forms stars, and increases the O abundance. With feedback from SNe turned off, small galaxies produce too many metals too early at the expense of their cold gas content, producing  $M_*$ - $Z$  and  $y_{eff}$ - $M_{bar}$  relations too flat compared to observations, in agreement with some early theoretical predictions (De Rossi et al. 2006; Dalcanton 2006). SN feedback prevents low mass galaxies from enriching their gas to a high metallicity at all redshifts. In our runs, star formation in small field galaxies occurs over extended periods of time until the present, in agreement with observations (Dolphin et al. 2005).

We would like to thank Chris Brook, Henry Lee, Evan Skillman, Kim Venn, Julianne Dalcanton, Andrey Kravtsov, and Andrew West for helpful conversations during this project. Support for this work, part of the Spitzer Space Telescope Theoretical Research Program, was provided by NASA through a contract issued by the

Jet Propulsion Laboratory under a contract with NASA. FG acknowledges support from NSF grant AST-0098557. Simulations were run at the Pittsburgh Supercomputing Center, SDSC, and Cineca. AB,GS, and TQ were supported by NSF ITR grant PHY-0205413.

## REFERENCES

- Dalcanton, J. J. 2006, astro-ph/0608590  
Dalcanton, J. J., Yoachim, P., & Bernstein, R. A. 2004, *ApJ*, 608, 189  
Davé, R., Finlator, K., & Oppenheimer, B. D. 2006, astro-ph/0608537  
De Rossi, M. E., Tissera, P. B., & Scannapieco, C. 2006, astro-ph/0609243  
Dekel, A., & Birnboim, Y. 2006, *MNRAS*, 368, 2  
Dolphin, A. E., Weisz, D. R., Skillman, E. D., & Holtzman, J. A. 2005, astro-ph/0506430  
Efstathiou, G. et al. 2002, *MNRAS*, 330, L29  
Erb, D. K., Shapley, A. E., Pettini, M., Steidel, C. C., Reddy, N. A., & Adelberger, K. L. 2006, *ApJ*, 644, 813  
Geha, M., Blanton, M. R., Masjedi, M., & West, A. A. 2006, astro-ph/0608295  
Gill, S. P. D., Knebe, A., & Gibson, B. K. 2004, *MNRAS*, 351, 399  
Giovannelli, R., Haynes, M. P., Herter, T., Vogt, N. P., da Costa, L. N., Freudling, W., Salzer, J. J., & Wegner, G. 1997, *AJ*, 113, 53  
Governato, F., Willman, B., Mayer, L., Brooks, A., Stinson, G., Valenzuela, O., Wadsley, J., & Quinn, T. 2006, astro-ph/0602351  
Haardt, F., & Madau, P. 1996, *ApJ*, 461, 20  
Katz, N., & White, S. D. M. 1993, *ApJ*, 412, 455  
Kauffmann, G., White, S. D. M., & Guiderdoni, B. 1993, *MNRAS*, 264, 201  
Kennicutt, Jr., R. C. 1998, *ApJ*, 498, 541  
Kereš, D., Katz, N., Weinberg, D. H., & Davé, R. 2005, *MNRAS*, 363, 2  
Knebe, A., Green, A., & Binney, J. 2001, *MNRAS*, 325, 845  
Kobayashi, C., Springel, V., & White, S. D. M. 2006, astro-ph/0604107  
Kroupa, P., Tout, C. A., & Gilmore, G. 1993, *MNRAS*, 262, 545  
Lee, H., Skillman, E. D., Cannon, J. M., Jackson, D. C., Gehrz, R. D., Polomski, E. F., & Woodward, C. E. 2006, *ApJ*, 647, 970  
MacArthur, L. A., Courteau, S., Bell, E., & Holtzman, J. A. 2004, *ApJS*, 152, 175  
Martin, C. L., & Kennicutt, Jr., R. C. 2001, *ApJ*, 555, 301  
McGaugh, S. S. 2005, *ApJ*, 632, 859  
Moore, B., Ghigna, S., Governato, F., Lake, G., Quinn, T., Stadel, J., & Tozzi, P. 1999, *ApJ*, 524, L19  
Okamoto, T., Eke, V. R., Frenk, C. S., & Jenkins, A. 2005, *MNRAS*, 363, 1299  
Perlmutter, S. et al. 1997, *ApJ*, 483, 565  
Pettini, M. 2006, astro-ph/0603066  
Raiteri, C. M., Villata, M., & Navarro, J. F. 1996, *A&A*, 315, 105  
Robertson, B., Bullock, J. S., Cox, T. J., Di Matteo, T., Hernquist, L., Springel, V., & Yoshida, N. 2006, *ApJ*, 645, 986  
Savaglio, S. et al. 2005, *ApJ*, 635, 260  
Stinson, G., Seth, A., Katz, N., Wadsley, J., Governato, F., & Quinn, T. 2006, astro-ph/0602350  
Tassis, K., Kravtsov, A. V., & Gnedin, N. Y. 2006, astro-ph/0609763  
Thielemann, F.-K., Nomoto, K., & Yokoi, K. 1986, *A&A*, 158, 17  
Tinsley, B. M. 1980, *Fundamentals of Cosmic Physics*, 5, 287  
Tremonti, C. A. et al. 2004, *ApJ*, 613, 898  
Veilleux, S., Cecil, G., & Bland-Hawthorn, J. 2005, *ARA&A*, 43, 769  
Verde, L., Oh, S. P., & Jimenez, R. 2002, *MNRAS*, 336, 541  
Wadsley, J. W., Stadel, J., & Quinn, T. 2004, *New Astronomy*, 9, 137  
Weaver, T. A., & Woosley, S. E. 1993, *Phys. Rep.*, 227, 65  
West, A. A. 2005, Ph.D. Thesis  
White, S. D. M., & Frenk, C. S. 1991, *ApJ*, 379, 52  
Woosley, S. E., & Weaver, T. A. 1995, in *AIP Conf. Proc.* 327: *Nuclei in the Cosmos III*, ed. M. Busso, C. M. Raiteri, & R. Gallino, 365–+